

Determination of Catalytic Rate Constants in the Reaction of Lysozyme and Oligosaccharide by Computer Simulation Analysis

Hiroko TADA and Toshiaki KAKITANI*

Department of Physics, Kyoto University, Kyoto 606

*Research Institute for Fundamental Physics, Kyoto University, Kyoto 606

(Received July 20, 1972)

We have developed Chipman's kinetic study on a reaction of lysozyme and oligosaccharide. That is, we have analyzed how each catalytic rate constant affects the pattern of time-course graphs of oligomer concentrations in the reaction. By fitting computer simulation curves to three experimental time-course graphs, values of the catalytic rate constants for the bond-cleavage, transglycosylation and hydration are determined step by step. Also some binding constants are evaluated.

Recently Chipman formulated a kinetic model for the reaction of lysozyme and oligosaccharides including reaction mechanisms of hydrolysis and transglycosylation.¹⁾ The kinetic equations became much complicated, far from that of Michaelis-Menten type. Numerically solving them by computer, he rather well simulated experimental data²⁾ of the time-course graphs of oligomer concentrations in the reaction. Performing the least-squares fit to one of the experimental data, he evaluated the rate constant of bond-cleavage and the ratio between the rate constant of transglycosylation and that of hydration as 1.75 sec^{-1} and $2.77 \times 10^3 \text{ M}^{-1}$, respectively. This study is much valuable because a kinetic scheme which includes the transfer reaction is formulated in a simple form, and the value of the rate constant of bond-cleavage is given for the first time. In this paper, we intend to develop his study and determine the values of the rate constants of transglycosylation and hydration which are not determined by him. We do this by analyzing the role of each catalytic rate constant in the pattern of the time-course graph. In the next section, we briefly formulate our kinetic model which differs a little from Chipman's.

Kinetic Model

Lysozyme has six binding sites for the substrate (GlcNAc-MurNAc)_n³⁾ named A, B, C, D, E, and F, and it cleaves the glycosyl bond locating between the D and E sites of the bound substrate.⁴⁾ As MurNAc cannot be bound at the A, C, and E sites, the oligomer is cleaved only between MurNAc and GlcNAc.⁵⁾ Therefore, in the kinetic treatment, we can consider the disaccharide GlcNAc-MurNAc as a unit. Then, six species of binding forms are allowed. In Fig. 1 we show our kinetic model. The notation is as follows: D_n is the oligomer (GlcNAc-MurNAc)_n, $C_{n,i}$ the complex of D_n and the enzyme E where the i -th susceptible

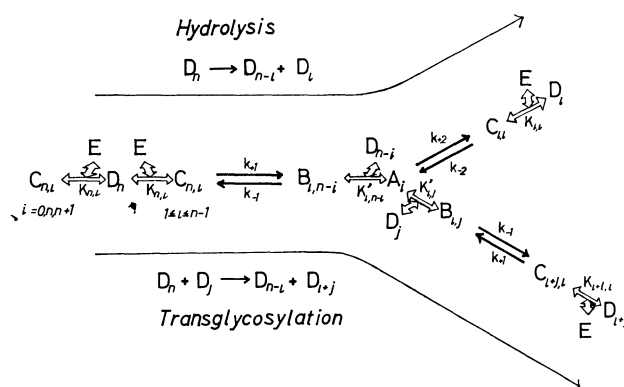


Fig. 1. Kinetic scheme of the lysozyme-catalyzed reaction. The notation is explained in the text.

bond from the non-reducing terminus of the oligosaccharide is at the catalytic site, A_i the "enzyme-carbonium ion intermediate" complex,⁴⁾ and $B_{i,n-i}$ the complex of A_i and D_n in which the non-reducing terminus of D_n is bound at the EF site of A_i . The complexes $C_{n,i}$ for $i=0, n, n+1$ are the non-productive ones, and $C_{n,i}$ for $1 \leq i \leq n-1$ are the productive ones. Catalytic rate-constants, k_{+1} , k_{-1} , k_{+2} , and k_{-2} are those of bond-cleavage, bond-formation, hydration and its reverse process, respectively. These catalytic rate constants are assumed to be same for both poor and good substrates. The arrow \xrightleftharpoons{K} represents a binding process, in which we assume an equilibrium is attained. The binding constant is written beside the arrow. These binding constants are explicitly written as follows:

$$\left. \begin{aligned} K_{1,0} &= K_{EF}, K_{1,1} = K_{CD}, K_{1,2} = K_{AB} \\ K_{n,0} &= K_{EF}, K_{n,1} = K_{C \sim F}, K_{n,n} = K_{A \sim D}, K_{n,n+1} = K_{AB} \\ &\text{for } n \geq 2 \\ K_{n,i} &= K_{A \sim F} \quad \text{for } n \geq 3, \leq 2i \leq n-1 \\ K'_{n,j} &= K_{EF} \quad \text{for all } j \text{ and } n. \end{aligned} \right\} \quad (1)$$

This kinetic model is much simplified by considering the following group S_n of the substrates and group I_j of the intermediates within which all species are combined to each other by the binding equilibrium processes:

$$[S_n] = [D_n] + \sum_i [C_{n,i}] + \sum_j [B_{j,n}], \quad (n=1, 2, \dots) \quad (2)$$

$$[I_j] = [A_j] + \sum_n [B_{j,n}], \quad (j=1, 2, \dots) \quad (3)$$

1) D. M. Chipman, *Biochemistry*, **10**, 1714 (1971).

2) D. M. Chipman, J. J. Pollock, and N. Sharon, *J. Biol. Chem.*, **243**, 487 (1968).

3) Abbreviation: GlcNAc, *N*-acetyl-D-glucosamine; MurNAc, *N*-acetyl-muramic acid. All oligosaccharides referred to are linked β -(1 \rightarrow 4), with the reducing terminus written to the right. We call (GlcNAc-MurNAc)_n as 2*n*-mer. Particularly those for $n=2, 3$, and 4 are named as tetramer, hexamer, and octamer, respectively.

4) D. C. Phillips, *Sci. Amer.*, **215**, 78 (1966).

5) N. Sharon, *Proc. Roy. Soc. Ser. B.*, **167**, 402 (1967).

The kinetic equations for these groups are written as

$$\frac{d[S_1]}{dt} = k_{+2}[A_1] - k_{-1}K_{EF}[D_1]\sum_j[A_j] + k_{+1}K_{C\sim F}[D_2][E] + k_{+1}K_{A\sim F}[E]\sum_{l>2}[D_l], \quad (4)$$

$$\begin{aligned} \frac{d[S_n]}{dt} = & k_{+2}[A_n] - k_{+1}\{K_{C\sim F} + (n-2)K_{A\sim F}\}[D_n][E] \\ & - k_{-1}K_{EF}[D_n]\sum_j[A_j] + k_{+1}K_{C\sim F}[D_{n+1}][E] \\ & + k_{+1}K_{A\sim F}[E]\sum_{l>n+1}[D_l] + k_{-1}K_{EF}\sum_{m<n}[A_m][D_{n-m}], \end{aligned}$$

for $n \geq 2$ (5)

$$\begin{aligned} \frac{d[I_j]}{dt} = & -k_{+2}[A_j] + k_{+1}K_j'[E]\sum_{l>j}[D_l] \\ & - k_{-1}K_{EF}[A_j]\sum_n[D_n], \quad (j=1, 2, \dots) \end{aligned} \quad (6)$$

where

$$[D_n] = [S_n]/(1 + K_n[E] + K_{EF}\sum_j[A_j]) \quad (7)$$

$$[A_j] = [I_j]/(1 + K_{EF}\sum_n[D_n]) \quad (8)$$

$$[E] = ([E]_0 - \sum_j[I_j])/(1 + \sum_n K_n[D_n]) \quad (9)$$

$$K_j' = \begin{cases} K_{C\sim F} & \text{for } j=1 \\ K_{A\sim F} & \text{for } j=2, \end{cases} \quad (10)$$

$$K_n = \sum_{i=0}^{n+1} K_{n,i} = \begin{cases} K_{EF} + K_{CD} + K_{AB} & \text{for } n=1 \\ K_{EF} + K_{C\sim F} + (n-2)K_{A\sim F} + K_{A\sim D} + K_{AB} & \text{for } n \geq 2 \end{cases} \quad (11)$$

In the above $[E]_0$ is the total enzyme concentration.

Here we mention about the difference between our model and Chipman's. Although our model is based on the consideration of the equilibrium at the binding process also for intermediates, Chipman's model is based on the scheme of the two-step enzymic reaction similar to α -chymotrypsin.⁶ That is, he neglected, in Fig. 1, all species of B and the complexes C at the exits of the catalytic processes. But this difference is trivial. Indeed, observed quantities of the time-course graphs are the percent radioactivity P_n defined by

$$P_n = 100n[S_n]/\sum_l l[D_l]_0, \quad (12)$$

where $l[D_l]_0$ is the initial substrate concentration of the l -mer measured by GlcNAc-MurNAc unit. Thus, the time-course graph perfectly coincides between both models if our $k_{-1}K_{EF}$ is put equal to Chipman's rate constant of transglycosylation k_T . If either the experiment by which one can detect the species of C or B , or the calculation without the equilibrium-assumption for the binding is made, small difference between the two models will appear.

Numerical Calculation

Experimentally it is shown that k_{-2} is much small compared with all other reaction rate constants.² Thus we neglect its process in the numerical calculation. The binding constants $K_{A\sim F}$, $K_{A\sim D}$, and K_{AB} will be equalized with the apparent binding constants experi-

mentally obtained for the hexamer, tetramer, and dimer, respectively. Those values are 3.5×10^4 , 2.0×10^3 , and 20 M^{-1} , respectively.⁷ If we use the additivity-assumption of the binding energy, $K_{C\sim F}$, K_{CD} , and K_{EF} are calculated from the above binding constants as 28, 1.6, and 0.3 M^{-1} , respectively. However, the validity of the additivity-assumption has been proved neither experimentally nor theoretically. Therefore, we treat $K_{C\sim F}$, K_{CD} , and K_{EF} as unknown parameters together with k_{+1} , k_{-1} , and k_{+2} . In the following, we call a reaction, where the $2m$ -mer is initially mixed with

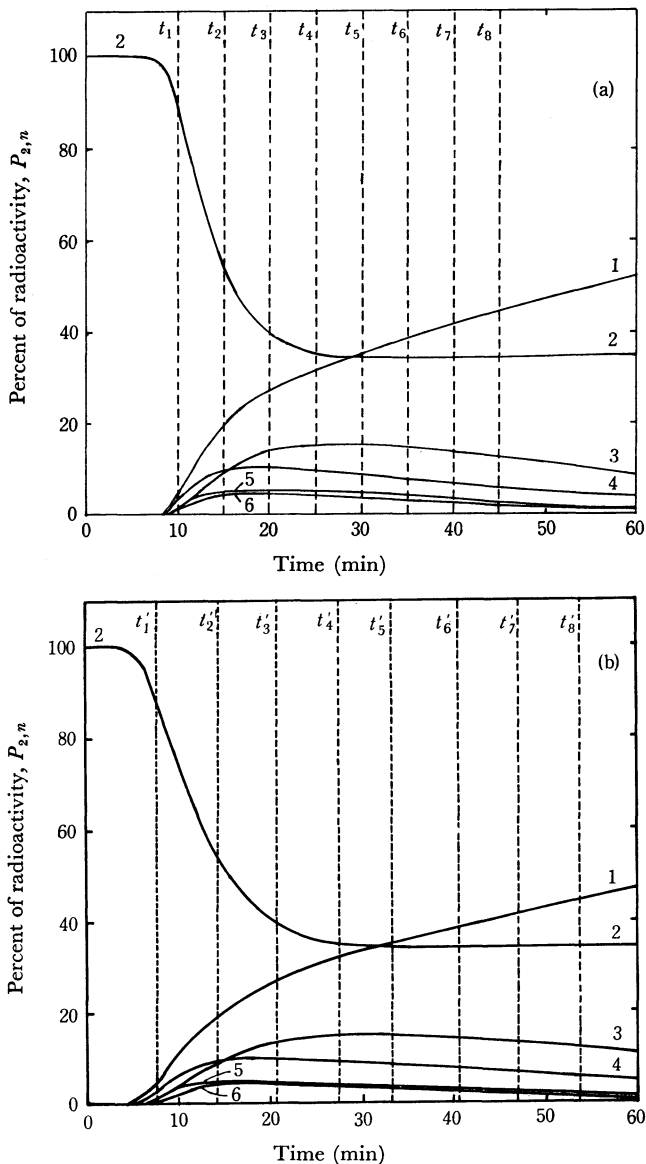


Fig. 2. Comparison of two time-course graphs in the tetramer-reaction between which the value of a is the same but those of the other kinetic constants are not. (a): $k_{+1} = 2.0 \text{ sec}^{-1}$, $k_{-1} = 1.8 \times 10^3 \text{ sec}^{-1}$, $k_{+2} = 0.62 \text{ sec}^{-1}$, $K_{C\sim F} = 2 \times 10^{-4} \text{ M}^{-1}$, $K_{CD} = 1.6 \text{ M}^{-1}$ and $K_{EF} = 1.0 \text{ M}^{-1}$. (b): $k_{+1} = 1.7 \text{ sec}^{-1}$, $k_{-1} = 3.3 \times 10^3 \text{ sec}^{-1}$, $k_{+2} = 0.33 \text{ sec}^{-1}$, $K_{C\sim F} = 5.0 \text{ M}^{-1}$, $K_{CD} = 1.6 \text{ M}^{-1}$ and $K_{EF} = 3.0 \text{ M}^{-1}$. The value of a is $3.0 \times 10^3 \text{ M}^{-1}$ for both (a) and (b). The initial condition is $[D_2]_0 = 7.5 \times 10^{-3} \text{ M}$, $[E]_0 = 2.1 \times 10^{-5} \text{ M}$. The number beside each curve is the value of n .

6) M. L. Bender and F. J. Kézdy, *J. Amer. Chem. Soc.*, **86**, 3704 (1964).

7) D. M. Chipman, V. Grisaro, and N. Sharon, *J. Biol. Chem.*, **242**, 4388 (1967).

lysozyme, as the $2m$ -mer reaction. In our numerical calculation, the maximum length of the oligomer is put to be 18-mer. However, for example, in the tetramer-reaction, the largest oligomer given in the experimental curves is $P_{2,6}$. In such a case, we put $P_{2,6} = \sum_{n=6}^9 P_{2,n}$ in our calculation. For the hexamer and octamer-reactions, we employed the similar procedure.

From the inspection of many time-course graphs with different values of the parameters, we have found the following important properties in this kinetic model. (i) In Fig. 2, we plotted two graphs of the tetramer-reaction, between which the ratio $a = k_{-1}K_{EF}/k_{+2}$ is same but the values of k_{+1} , k_{+2} , $K_{C \sim F}$, and K_{CD} are not same. In Fig. 2(a), we pick up an arbitrary set of times $\{t_i\}$ ($i=1, 2, \dots, N$), and obtain $\{P_{2,n}^a(t_i)\}$, where $P_{2,n}^a(t_i)$ denotes $P_{2,n}$ at time t_i in Fig. 2(a). Then, we find a set of times $\{t_i'\}$ which nicely satisfy the equation

$$P_{2,n}^b(t_i') = P_{2,n}^a(t_i) \quad (13)$$

for all n in Fig. 2(b) irrespectively of the values of the other parameters. This means that the ratio a is an essential factor which determines the distribution of the oligomer concentrations. This property holds also in the hexamer- and octamer-reactions. In the next section, we shall qualitatively explain this important property of our kinetic model. (ii) The time scale of the reaction is determined mainly by the catalytic rate constants k_{+1} and k_{+2} . But they do not necessarily change the time scale uniformly. (iii) As shown in Fig. 3, the binding constant $K_{C \sim F}$ plays a role only in the initial stage called "time-lag-region" of the tetramer-reaction and little affects the time-course graphs of the

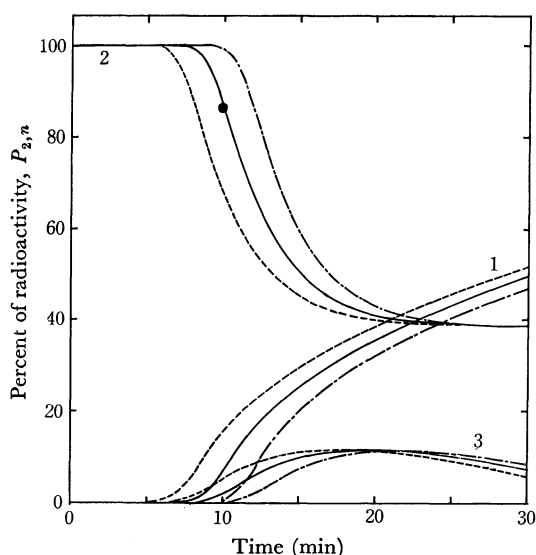


Fig. 3. Time-course graphs of the tetramer-reaction where the value of $K_{C \sim F}$ is varied. —: $K_{C \sim F} = 10^{-5} \text{ M}^{-1}$, —: $K_{C \sim F} = 10^{-7} \text{ M}^{-1}$, - - -: $K_{C \sim F} = 10^{-9} \text{ M}^{-1}$. The other parameters are $k_{+1} = 3.3 \text{ sec}^{-1}$, $k_{-1} = 9.8 \times 10^2 \text{ sec}^{-1}$, $k_{+2} = 0.58 \text{ sec}^{-1}$, $K_{CD} = 1.6 \text{ M}^{-1}$ and $K_{EF} = 1.0 \text{ M}^{-1}$. The initial concentrations of D_2 and E are the same as those in Fig. 2. The black circle is the experimental value of $P_{2,2}$ at 10 min.²⁾ The number beside each curve is the value of n . Curves of oligomers higher than hexamer are not written in this graph.

hexamer- and octamer-reactions. This property comes from the fact that the tetramer is a poor substrate although the higher oligomer is a good substrate.²⁾ (iv) The binding constant K_{EF} affects the time-course graphs only through the form of $k_{-1}K_{EF}$ except when k_{EF} is much larger than K_{AB} . This is easily understood from the fact that K_{EF} enters into the kinetic equations mainly by the form of $k_{-1}K_{EF}$. This property states that we cannot simply determine the value of k_{-1} and K_{EF} independently. (v) The binding constant K_{CD} does not affect our time-course graphs unless K_{CD} is much larger than K_{AB} .

Determination of the Ratio $a = k_{-1}K_{EF}/k_{+2}$. In fitting of the theoretical curves to the experiments, we use the experimental values in the early stage of the reaction, because our kinetic model may not be good in the latter stage of the reaction as we discuss later. In the following numerical calculation, we used the times $t_1 = 10 \text{ min}$ and $t_2 = 17 \text{ min}$ for the tetramer-reaction, and $t_1 = 1 \text{ min}$ and $t_2 = 4 \text{ min}$ for the hexamer- and octamer-reactions.

Using the property (i), we can determine the value of the parameter a by best fitting the theoretical curve to the experimental values $P_{m,n}^E(t_1)$ and $P_{m,n}^E(t_2)$ for all n in the three reactions, where the superscript E denotes the experiment. We describe below the method of our calculation. First we fix the value of a . Suitably choosing the other parameters, we obtain t_1' 's and t_2' 's which satisfy the equation

$$P_{m,n}(t_i') = P_{m,n}^E(t_i), \quad (i=1, 2) \quad (14)$$

for the tetramer-, hexamer-, and octamer-reactions, respectively. Then we calculate the following error function:

$$f_{m,i}(a) = \sum \{P_{m,n}(t_i') - P_{m,n}^E(t_i)\}^2, \quad (i=1, 2) \quad (15)$$

Error functions thus obtained depend on a and are plotted in Fig. 4. The sum of these six error functions becomes minimum at $a = 1.7 \times 10^3 \text{ M}^{-1}$. This minimum point is determined mainly by the three $f_{m,2}$'s. But we should not trust this value so firmly, because the minimum points in error function largely differ from each other. It will be right to say that the value of a is roughly in the region $1.2 \times 10^3 \text{ M}^{-1} < a < 4.0 \times 10^3 \text{ M}^{-1}$.

Determination of k_{+1} and k_{+2} . The values of k_{+1} and k_{+2} are not determined uniquely from the fitting procedure to a single kind of reaction, but only a functional relationship between them is obtained. Using the property (ii), we intend to obtain sets of k_{+1} and k_{+2} in each reaction for the fixed value of a . In the tetramer-reaction, the set of k_{+1} and k_{+2} are obtained by the procedure that t_1' and t_2' , which are obtained from Eq. (14), may satisfy $t_2' - t_1' = t_2 - t_1 = 7 \text{ min}$. For the hexamer- and octamer-reactions, they are determined as the average of those which satisfy $t_1' = t_1 = 1 \text{ min}$ and $t_2' = t_2 = 4 \text{ min}$, respectively. The obtained values k_{+1} and k_{+2} are shown in Fig. 5 for two values of a . Our expectation was that the three curves should cross at a point, which determines the real values of k_{+1} and k_{+2} . Indeed, it is well realized. From this graph, we obtain $k_{+1} = 3.3 \text{ sec}^{-1}$ and $k_{+2} = 0.58 \text{ sec}^{-1}$ for $a = 1.7 \times 10^3 \text{ M}^{-1}$, and $k_{+1} = 2.0 \text{ sec}^{-1}$ and $k_{+2} = 0.62 \text{ sec}^{-1}$

TABLE 1. VALUES OF THE KINETIC CONSTANTS

The free energy of the catalytic rate constant is calculated from the equation $\Delta F^\ddagger_x = -RT \ln (k_x h / \kappa T)$.
The cooperative energy E_c is also listed.

Kinetic constants	Ours $a=1.7 \times 10^3 \text{M}^{-1}$	Ours $a=3.0 \times 10^3 \text{M}^{-1}$	Chipman's ¹⁾ $a=2.77 \times 10^3 \text{M}^{-1}$
k_{+1} (sec ⁻¹)	3.3	2.0	1.75
$k_{-1}K_{\text{EF}}$ (M ⁻¹ sec ⁻¹)	9.8×10^2	1.8×10^3	Unknown (9.2×10^4)
k_{+2} (sec ⁻¹)	0.58	0.62	Unknown (1.0×10^2)
$K_{\text{C}\sim\text{F}}$ (M ⁻¹)	10^{-7}	2×10^{-4}	$\leq 6.3 \times 10^{-4}$
K_{CD} (M ⁻¹)	5.7×10^{-8}	1.2×10^{-5}	(0.5)
K_{EF} (M ⁻¹)	Unknown	Unknown	Unknown
ΔF^\ddagger_{+1} (kcal/mol)	17.0	17.2	17.4
$\Delta F^\ddagger_{-1} + \Delta F_{\text{EF}}$ (kcal/mol)	13.5	13.1	(10.8)
ΔF^\ddagger_{+2} (kcal/mol)	18.0	17.9	(14.9)
$\Delta F_{\text{C}\sim\text{F}}$ (kcal/mol)	9.7	5.1	≥ 4.4
ΔF_{CD} (kcal/mol)	10.0	6.8	(0.4)
E_c (kcal/mol)	11.8	7.2	≥ 6.5

The values in the parentheses are the standard values of Chipman.

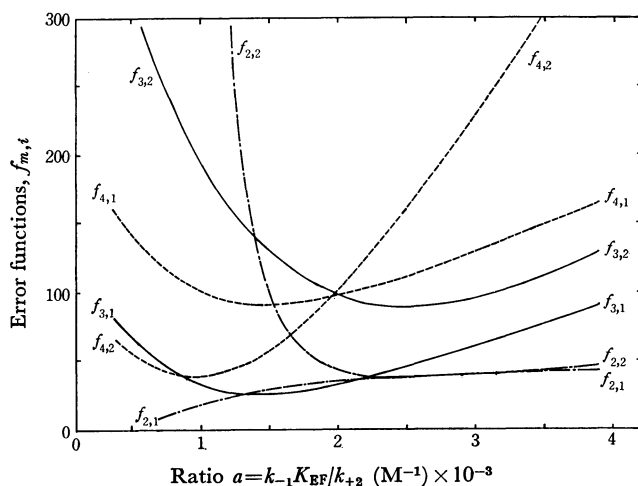


Fig. 4. Graphs of error-functions. ---: tetramer-reaction, —: hexamer-reaction and -·-·: octamer-reaction. The initial conditions used for our calculation are as follows: In the tetramer-reaction $[D_2]_0 = 7.5 \times 10^{-3} \text{M}$ and $[E]_0 = 2.1 \times 10^{-5} \text{M}$. In the hexamer-reaction $[D_3]_0 = 2.9 \times 10^{-4} \text{M}$ and $[E]_0 = 2.0 \times 10^{-6} \text{M}$. In the octamer-reaction $[D_4]_0 = 2.4 \times 10^{-4} \text{M}$ and $[E]_0 = 2.0 \times 10^{-6} \text{M}$.

for $a = 3.0 \times 10^3 \text{M}^{-1}$.

Determination of $K_{\text{C}\sim\text{F}}$. We use the property (iii). As shown in Fig. 3, we determine the value of $K_{\text{C}\sim\text{F}}$ in such a way that $P_{2,2}$ may pass $P_{2,2}^E(t_1)$, fixing all the other parameters, where $t_1 = 10$ min. Some theoretical curves for the case of $a = 1.7 \times 10^3 \text{M}^{-1}$ are plotted in Fig. 3. From this, we get $K_{\text{C}\sim\text{F}} = 10^{-7} \text{M}^{-1}$. In the same way, we get $K_{\text{C}\sim\text{F}} = 2 \times 10^{-4} \text{M}^{-1}$ for the case of $a = 3.0 \times 10^3 \text{M}^{-1}$.

In Table 1, we summarized our results, together with the value of Chipman.¹⁾ The method to get the value of K_{CD} is written in the following section. In Fig. 6, theoretical curves of ours are drawn and compared with the experiment.

Theoretical Analysis and Discussion

At first, we consider the important qualitative charac-

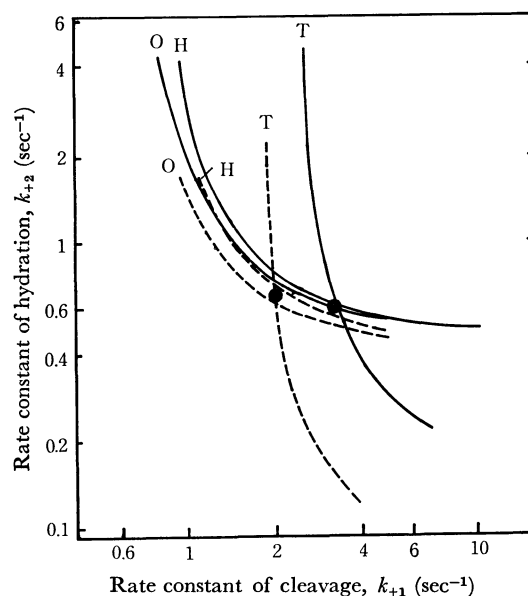


Fig. 5. Graphs of the sets of k_{+1} and k_{+2} . —: $a = 1.7 \times 10^3 \text{M}^{-1}$ and -·-·: $a = 3.0 \times 10^3 \text{M}^{-1}$. The letters T, H, and O denote the tetramer-, hexamer- and octamer-reactions, respectively. The black circles are our obtained points through which three curves pass.

teristics of our kinetic model. The most important one is the property (i), i.e., the distribution of oligomers is almost uniquely determined by the ratio $a = k_{-1}K_{\text{EF}}/k_{+2}$. The reduced scheme of the reaction-path of this kinetic model is represented by the groups of the substrates and the intermediates as in Fig. 7, which is called as Path(n, i) henceforth. In the Path(n, i), if the step X(n, i) is rate-determining, the intermediate is rapidly converted to each product through the step Y(i). Then, on a given iteration step, a decrease of ΔC moles in S_n through the Path(n, i) produces the change ΔS_m in S_m . From Eqs. (5) and (6) it is given by

$$\Delta S_m = d_m - d_{i+m} + (\delta_{m,n-i} - \delta_{m,n}) \cdot \Delta C, \quad (m=1, 2, \dots) \quad (16)$$

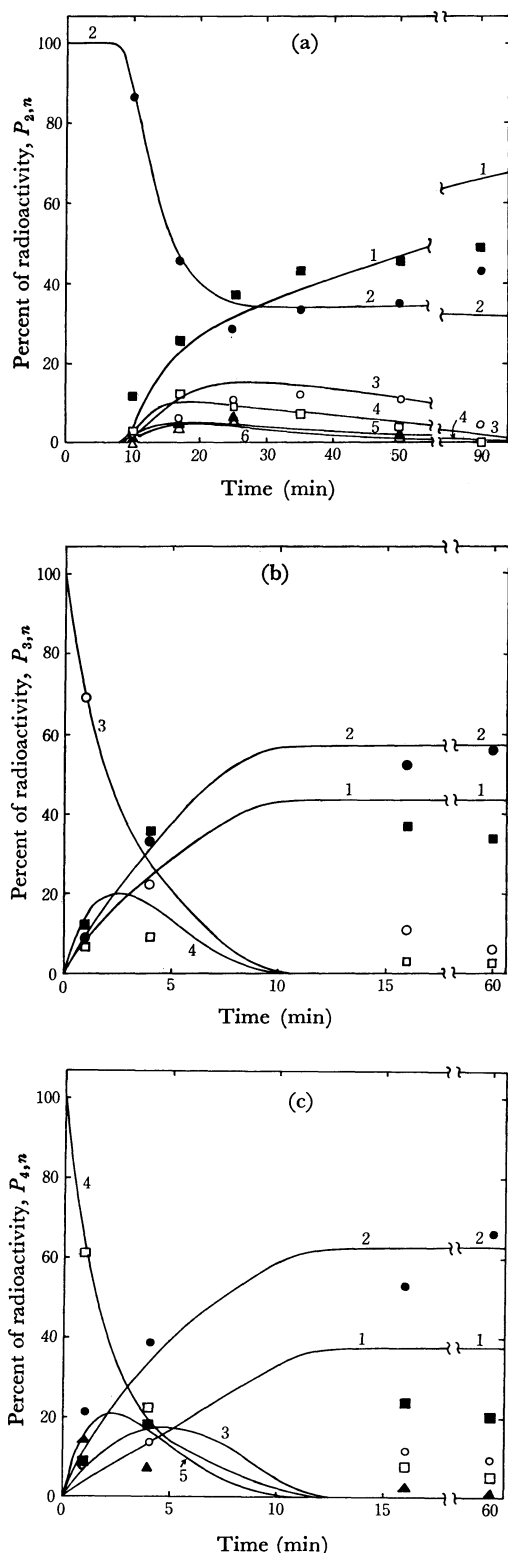


Fig. 6. Theoretical time-course graphs compared with the experiment. (a), (b), and (c) are the graphs of the tetramer-, hexamer- and octamer-reactions. The kinetic constants are as follows: $k_{+1}=2.0 \text{ sec}^{-1}$, $k_{-1}=1.8 \times 10^3 \text{ sec}^{-1}$, $k_{+2}=0.62 \text{ sec}^{-1}$, $K_{C-F}=2 \times 10^{-4} \text{ M}^{-1}$, $K_{CD}=1.6 \text{ M}^{-1}$ and $K_{EF}=1.0 \text{ M}^{-1}$. The initial concentrations of the oligomer and the enzyme are same as those in the figure legend of Fig. 4. The experimental points²⁾ are shown by the following symbols; \blacksquare : dimer, \bullet : tetramer, \circ : hexamer, \square : octamer, \blacktriangle : 10-mer, \triangle : 12-mer. The number beside each curve is the value of n .

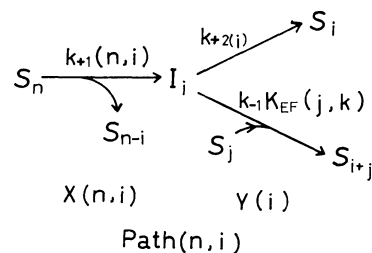


Fig. 7. The reduced scheme of the reaction-path. The step $X(n,i)$ is the process of the bond-cleavage of the $2n$ -mer in the productive i -th binding form and the step $Y(i)$ is the process where the carbonium intermediate is converted to an oligomer of different kind depending on the species of the acceptor. The reduced catalytic rate constants in this figure are defined by $k_{+1}(n,i)=k_{+1}K_{n,i}[E]/(1+K_n[E]+K_{EF}\sum_l[A_l])$, $k_{+2}(i)=k_{+2}/(1+K_{EF}\sum_l[D_l])$ and $k_{-1}K_{EF}(j,k)=k_{-1}K_{EF}/\{(1+K_{EF}\sum_l[D_l])(1+K_j[E]+K_{EF}\sum_l[A_l])\}$.

where

$$d_m = \begin{cases} 0 & \text{for } m < i \\ \Delta C/(1+a\sum_l[D_l]) & \text{for } m = i \\ \Delta C \cdot a \cdot [D_{m-i}]/(1+a\sum_l[D_l]) & \text{for } m > i \end{cases} \quad (17)$$

and δ_{ij} is the Kronecker's delta function. In Eqs. (16) and (17), as $\{[D_l]\}$ are given from the previous step of the iteration procedure, ΔS_m is uniquely determined by a . Since the total reaction is obtained as the sum of this $\text{Path}(n,i)$ over n and i , the total change on this iteration step is also uniquely determined by a . The time-course graphs are obtained by accumulating these iteration steps. Thus the pattern of the distribution is uniquely determined by a . When the step $Y(i)$ is rate-determining, the situation is more complicated. Among the groups $\{S_m\}$ ($m=i, i+1, \dots$) directly produced by the step $Y(i)$, the productive complexes $\{C_{m,l}\}$ ($m=i, i+1, \dots; l=1, 2, \dots, m-1$) are immediately converted to $\{S_{m-l}\}$ and $\{I_l\}$ through the steps $\{X(m,l)\}$, and further these products $\{S_{m-l}\}$ pass the same procedure as $\{S_m\}$. Then the changes in S_m and I_m due to a decrease of ΔC moles in I_i through the step $Y(i)$ is obtained, accumulating also the effects of these sequential steps, as follows:

$$\Delta S_m = -d_{i+m} + Z_m\{d_m + d_{m+1}Z_{m+1,m} + \sum_{n>m+1} d_n(Z_{n,m} + \sum_{k=1}^{n-m-1} \sum_{\{n>l_1>l_2>\dots>l_k>m\}} Z_{n,l_1}Z_{l_1,l_2}\dots Z_{l_k,m})\} \quad (18)$$

$$\Delta I_m = -\delta_{i,m}\Delta C + \sum_{n>m} d_n[Z_{n,n-m} + (1-\delta_{n,m+1}) \times \sum_{k=1}^{n-m-1} Z_{k+m,k}\{Z_{n,k+m} + (1-\delta_{k,n-m-1}) \times \sum_{j=1}^{n-k-m-1} \sum_{\{n>l_1>l_2>\dots>l_j>k+m\}} Z_{n,l_1}Z_{l_1,l_2}\dots Z_{l_j,k+m}\}], \quad (19)$$

where

$$Z_m = \{1 + (K_{EF} + K_{m,m} + K_{m,m+1})[E] + K_{EF}\sum_l[A_l]/(1 + K_m[E] + K_{EF}\sum_l[A_l])\} \\ Z_{m,j} = K_{m,m-j}[E]/(1 + K_m[E] + K_{EF}\sum_l[A_l]) \quad (20)$$

and $\{d_m\}$ are the same as Eq. (17). The sum of $\{n>l_1>l_2>\dots>l_k>m\}$ denotes to sum up for all the set of l_1, l_2, \dots, l_k satisfying the relation in the parentheses. In Eq. (20), $[E]$ and $\{[A_i]\}$ are given from the previous step of the iteration procedure. Then, also in this case, the distribution of oligomers is uniquely determined by a . When both the steps $X(n,i)$ and $Y(i)$ are rate-determining, the same conclusion may be obtained approximately although the exact explanation is impossible. The other important qualitative characteristic of our model is that; the time scale of the time-course graphs is determined only by the rate constants of the rate-determining steps independently of the other rate constants. When every step is rate-determining, it is dependent on all rate constants. Then, as shown in Fig. 5, the values of k_{+1} and k_{+2} with which the calculated graphs fit to a single time-course graph of the experiment are of the hyperbolic-like relation. These two conclusions are the general qualitative aspects in the endocatenase-catalyzed reaction of oligomers involving the transfer-reaction.

Next we compare our calculation with that of Chipman.¹⁾ Using the method of the least-squares fit to 24 data points of the tetramer-reaction, he obtained the following results: (a) k_{+1} is rate-determining and its value is $(1.75 \pm 0.17) \text{ sec}^{-1}$, (b) the value of a is $(2.77 \pm 0.3) \times 10^3 \text{ M}^{-1}$, (c) $k_{-1}K_{EF}$ and k_{+2} are not rate-determining, thus those values are not obtained, and (d) the value of $K_{C \sim F}$ is less than $(6.3 \pm 12.4) \times 10^{-4} \text{ M}^{-1}$. His values of a and k_{+1} are rather in agreement with ours. But, his results, (b) and (c), do not seem to be correct judging from our graph of Fig. 5. That is, the tetramer curve in Fig. 5 is almost perpendicular at $k_{+1} \cong 1.8 \text{ sec}^{-1}$ and bends to the right as the value of k_{+1} becomes larger than 2.0 sec^{-1} . Thus, k_{+1} is not rate-determining except the perpendicular region of the curve. This means that one cannot determine the values of k_{+1} or k_{+2} but obtain a relation between them from the data of the tetramer-reaction only.¹⁰⁾ In our calculation, we used other two data, i.e., time-course graphs of the hexamer- and octamer-reactions. Finding the cross points among these three curves, we succeeded in determining the values of k_{+1} and k_{+2} . The point corresponding to his standard values lies near the upper-extrapolated tetramer curve, but far above the hexamer and octamer curves in Fig. 5. There may be an argument that the experiments of the hexamer- and octamer-reactions are not so correct.⁹⁾ If it is really so, our results will also be corrected. But, our procedure to determine the values of the catalytic rate constants using graphs similar to Fig. 5 is useful whenever other reliable experiments appear. As to the value of $K_{C \sim F}$, our result is consistent with his.

Summarizing the above results and using the value of the free-energy of the hydrolysis of maltose,⁹⁾ which is similar to that of MurNAc-GlcNAc, we give in

8) D. M. Chipman, private communication.

9) R. A. Dedonder, *Ann. Rev. Biochem.*, **30**, 347 (1961).

10) Examining reactions of higher oligosaccharides under low concentration conditions, Chipman seems to have estimated that k_{+2} should be at least of the order of 0.5 sec^{-1} . If it is assumed, his results (b) and (c) are derived.

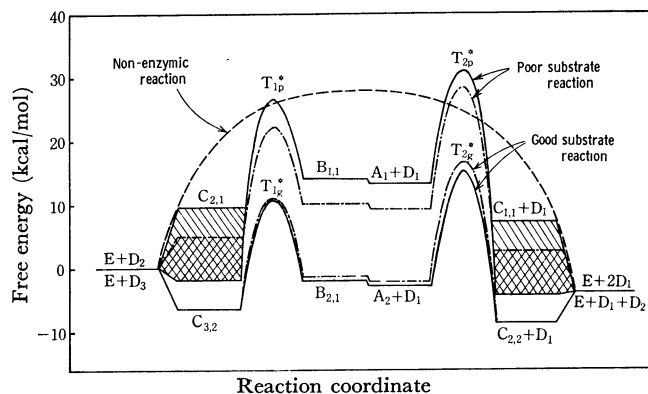


Fig. 8. Free-energy scheme in the lysozyme-catalyzed reaction. The graphs of the tetramer- and hexamer-reactions are written together by fitting the initial energy levels to zero. —: $a = 1.7 \times 10^3 \text{ M}^{-1}$, - - - : $a = 3.0 \times 10^3 \text{ M}^{-1}$. The energy levels of $C_{2,1}$ and $C_{1,1} + D_1$ have uncertainty. The highest levels of them are those obtained from the assumption that the catalytic rate constants are same for both the good and poor substrates. The lowest levels are those obtained from the additivity-assumption of the binding energy. The real energy levels will be between those of the two extreme cases. These graphs are written assuming $K_{EF} = 0.3 \text{ M}^{-1}$. When this value is altered, the energy levels of $B_{1,1}$ and $B_{2,1}$ shift by $-RT \ln(K_{EF}/0.3) \text{ kcal/mol}$, keeping all the other energy levels unchanged. T_{1p}^* , T_{2p}^* , T_{1g}^* , T_{2g}^* represent transition states for the poor and good substrates reactions. The energy level of the non-enzymic reaction is also written for comparison.

Fig. 8 a schematic model for the free-energy potential of lysozyme reaction. From the case of the good substrates in Fig. 8, the value of k_{-2} is estimated as about 10^{-4} sec^{-1} , which is much smaller than the other catalytic rate constants as expected. Furthermore, the unknown binding constant K_{CD} is estimated by the difference between the energy height of T_{2p}^* from the line $E + 2D_1$ and that of T_{2g}^* from the line $C_{2,2} + D_1$, as $1.2 \times 10^{-5} \text{ M}^{-1}$ and $5.7 \times 10^{-8} \text{ M}^{-1}$ for $a = 3.0 \times 10^3 \text{ M}^{-1}$ and $1.7 \times 10^3 \text{ M}^{-1}$, respectively. The non-enzymic case is also drawn in Fig. 8 for comparison, using Piszkievicz and Bruice's data on the di-N-acetylchitobiose.¹¹⁾ The transition state for the poor substrates has almost the same height as the non-enzymic one, but, for the good substrates, it is largely lowered by as much as 12–13 kcal/mol, which makes the overall rate constant by about 10^9 times larger. This large stabilization of the transition-state is produced by the cooperative binding effect between the AB and C~F sites. Its cooperative energy is calculated as

$$E_c = -RT \ln (K_{AB}K_{C \sim F}/K_{A \sim F}) - \Delta F_m \quad (21)$$

where ΔF_m , which is due to the mixing entropy, is about 2.4 kcal/mol. Here, if the additivity-assumption of the binding energy holds, E_c becomes zero. Our value of E_c is 11.8 kcal/mol and 7.2 kcal/mol for $a = 1.7 \times 10^3 \text{ M}^{-1}$ and $3.0 \times 10^3 \text{ M}^{-1}$, respectively. This large value means that the sites A and B play an important role to stabilize the distorted conformation at the D site in the reaction of the good substrates, although the mechanism of it is yet unknown.

11) D. Piszkievicz and T. C. Bruice, *J. Amer. Chem. Soc.*, **90**, 5844 (1968).

It may be also considered, however, that the real reaction of the bond-cleavage of the poor substrates proceeds in the more loosely bound form with less strain (*i.e.* much larger value of $K_{C\sim F}$), and by much smaller value of k_{+1} , maintaining the value of $k_{+1}K_{C\sim F}$ as constant (in the kinetic equations (4)–(9), $K_{C\sim F}$ appears mainly in the form $k_{+1}K_{C\sim F}$). The real energy level of this loosely bound complex may be located somewhere in the hatched region of Fig. 8. Similar consideration may be applied to K_{CD} and k_{-2} for the dimer.

The observable effect of the transglycosylation does not appear until the ratio a becomes so large that the value of $k_{-1}K_{EF}[D]$ becomes comparable to that of k_{+2} . It is reasonable that the order of our obtained value of a is 10^3 M^{-1} , since the substrate concentration is order of 10^{-3} – 10^{-4} M in the experiments we used. This result means that the rate constant of the transfer-reaction may be rather large even for the case of other enzyme-catalyzed reactions, in which an effective transfer-reaction had not been detected experimentally. It may be detected, if the suitable initial concentration of the substrate is used, so that the transfer-reaction process becomes comparable to the competitive process.

Recently, using the transient NMR¹²⁾ and T -jump method,¹³⁾ the forward binding rate constants k_{+b} for GlcNAc, (GlcNAc)₂, and (GlcNAc)₃ are obtained as $3.5 \times 10^5 \text{ M}^{-1}\text{sec}^{-1}$, $3.6 \times 10^6 \text{ M}^{-1}\text{sec}^{-1}$, and $4.44 \times 10^6 \text{ M}^{-1}\text{sec}^{-1}$, respectively. We find that the binding rate $k_{+b}[D_n][E]$ is not necessarily much larger than the reaction rate $k_{+1}[C_{i,j}]$. Therefore, the equilibrium-assumption about the binding process may not be so

good. In the following we shortly examine how our kinetic schemes and simulated time-course graphs are altered if the dynamical process of the binding is effective. The binding constants of the above oligomers are 20 – 50 M^{-1} , $5 \times 10^3 \text{ M}^{-1}$, and $1.0 \times 10^5 \text{ M}^{-1}$, respectively.¹⁴⁾ Therefore, we find that the binding rate constant does not become large so much as the binding constant does as the oligomer becomes large. This tendency will also apply to the higher oligomers. In addition, binding rate constant of the productive binding may become very small because the D site of the complex must be distorted. From these, it is well expected that the number of the productive complex is much smaller than that calculated from the equilibrium-assumption when considerable numbers of small oligomers coexist. Then, the reaction proceeds much slowly. In the latter stage of the hexamer- and octamer-reactions where dimer and tetramer are considerably produced, the above case might be applied. In the experimental result, this seems to have happened (considerable amounts of the hexamer and octamer remain even at 15 min). In the earlier stage of the reaction, the dynamical binding effect, if exists, might be small.

We think that our kinetic model and treatment based on its qualitative characteristics described in this paper are a useful general method to determine the catalytic rate constants of the endocatenase-catalyzed reaction of oligomer including the transfer-reaction.

The authors wish to express their sincere thanks to Dr. H. Fukutome for valuable discussions and improving this manuscript. They also thank to Prof. D. M. Chipman for the critical comments.

12) B. D. Sykes and C. Parravano, *J. Biol. Chem.*, **244**, 3900 (1969).

13) D. M. Chipman and P. R. Schimmel, *ibid.*, **243**, 3711 (1968).

14) D. M. Chipman and N. Sharon, *Science*, **165**, 454 (1969).